Optical properties and electronic structure of α'-Na$_{1-x}$Ca$_x$V$_2$O$_5$

C. Presura,[1] D. van der Marel,[1] M. Dischner,[2] C. Geibel,[2] and R. K. Kremer[3]

[1]*Solid State Physics Laboratory, University of Groningen, Nijenborgh 4, 9747 AG Groningen, The Netherlands*
[2]*Max-Planck-Institut für Chemische Physik fester Stoffe, D-01187 Dresden, Germany*
[3]*Max-Planck-Institut für Festkörperforschung, Heisenbergstrasse 1, D-70569 Stuttgart, Germany*

The dielectric function of α'-Na$_{1-x}$Ca$_x$V$_2$O$_5$ ($0 \leq x \leq 20\%$) was measured for the a and b axes in the photon energy range 0.8–4.5 eV at room temperature. By varying the Ca concentration we control the relative abundancy of V^{4+} and V^{5+}. We observe that the intensity of the main optical absorption peak at 1 eV is proportional to the number of V^{5+} ions. This rules out the interpretation as a V^{4+} $d-d$ excitation, and it establishes that this is the on-rung bonding-antibonding transition.

I. INTRODUCTION

α'-Na$_{1-x}$Ca$_x$V$_2$O$_5$ belongs to the larger group of α' vanadium pentoxides, with the chemical formula AV$_2$O$_5$ (A=Li, Na, Ca, Mg, etc.).[1] Their structure is remarkably similar to that of the parent compound V$_2$O$_5$, which consists of layers of square pyramids of O surrounding a V^{+5} ion. The layers are kept together via weak forces, which account for the easy cleavage of this oxide along (001). The basic building blocks forming the V$_2$O$_5$ layers are parallel ladders of VO$_5$ pyramids. In AV$_2$O$_5$ the A atoms enter the space between the layers and act as electron donors for the V$_2$O$_5$ layers. In the case of α'-NaV$_2$O$_5$, every doped electron is shared between two V atoms. As a result the average valence of the V ions corresponds to V$^{+4.5}$. X-ray diffraction indicates that at room temperature all V ions are in the same mixed valence state.[2–4]

Partial substitution of the Na$^+$ with Ca^{2+} leaves the α' crystal structure intact, but alters the relative abundance of V^{4+} and V^{5+}, $N^{4+}:N^{5+}=(1+x):(1-x)$. In this paper we report spectroscopic ellipsometry measurements on α'-Na$_{1-x}$Ca$_x$V$_2$O$_5$ ($x=0$, 0.06, 0.15, and 0.20), in the energy range 0.8–4.5 eV. We employ the dependence of the optical spectra on the $N^{4+}:N^{5+}$ ratio to identify the main components in the optical spectra, which in turn we use to reveal the electronic structure of this material.

II. DETAILS OF SAMPLE PREPARATION AND EXPERIMENTAL SETUP

The crystals (CR8, 45 008, and 45 010) had dimensions of approximately 1, 2, and 0.3 mm along the a, b, and c axes, respectively. The samples 45 008 and 45 010 were prepared from NaVO$_3$ flux.[5] In a first step a mixture of Na$_2$CO$_3$ and V$_2$O$_5$ is heated up to 550 °C in air to form NaVO$_3$. In a second step the NaVO$_3$ is mixed with VO$_2$ in the ratio of 8:1 and then heated up to 800 °C in an evacuated quartz tube and cooled down at a rate of 1 K per hour. The excess NaVO$_3$ was dissolved in water. Then the doped samples were produced by substituting in the first step Na$_2$CO$_3$ by CaCO$_3$. The chemical composition of the samples has been determined using energy dispersive x-ray fluoresence microprobe measurements. The results showed that the real Ca content of some samples was smaller that the nominal one (with a factor of 0.75), and that position dependent variations of the Na

stoichiometry are below 2%. A standard spectroscopic ellipsometer was used to collect ellipsometric data in the range of 6000–35 000 cm^{-1} from the ab planes of the crystals using two different crystal orientations, and to measure normal incidence reflectivity spectra of the ac plane with the electric-field vector along the c direction.

III. DATA COLLECTION AND ANALYZES

We performed ellipsometric measurements on the (001) surfaces of the crystals both with the plane of incidence of the light along the a and the b axis. An angle of incidence θ, of 66°, was used in all experiments. Ellipsometry provides directly the amplitude and phase of the ratio of the reflectivity coefficients of p- and s-polarized light[6] $r_p(\omega)/r_s(\omega)$. For an anisotropic crystal with the three optical axes oriented along the surface normal ($p\perp$), perpendicular to the plane of incidence (s), and along the intersection of the plane of incidence and the surface ($p\|$), this ratio is related to the dielectric tensor elements along these three directions ($\epsilon_{p\perp}$, ϵ_s, and $\epsilon_{p\|}$) according to the expression

$$\frac{r_p}{r_s} = \frac{\sqrt{\epsilon_{p\|}\epsilon_{p\perp}}\cos\theta - \sqrt{\epsilon_{p\perp}-\sin^2\theta}}{\sqrt{\epsilon_{p\|}\epsilon_{p\perp}}\cos\theta + \sqrt{\epsilon_{p\perp}-\sin^2\theta}} \frac{\cos\theta + \sqrt{\epsilon_s - \sin^2\theta}}{\cos\theta - \sqrt{\epsilon_s - \sin^2\theta}}. \tag{1}$$

To extract the dielectric constant from the ellipsometric parameters we proceed in two steps: First the pseudodielectric functions along the optical axes are extracted from the ellipsometric data using the inversion formula

$$\epsilon_{p\|}^{ps} = \sin^2\theta\left[1 + \tan^2\theta\left(\frac{1-r_p/r_s}{1+r_p/r_s}\right)^2\right]. \tag{2}$$

For isotropic crystals this expression provides the dielectric function directly. The pseudo-dielectric function is close to the dielectric tensor elements along the intersection of the plane of incidence and the crystal surface.[7] A biaxial crystal like α'-NaV$_2$O$_5$ has three complex dielectric functions, ϵ_a, ϵ_b, and ϵ_c along each optical axis, and an ellipsometric measurement involves all three tensor components of the dielectric matrix. In addition to the pseudo-dielectric functions displayed Fig. 1(a), $\epsilon_c(\omega)$ is required. No ac or bc crystal
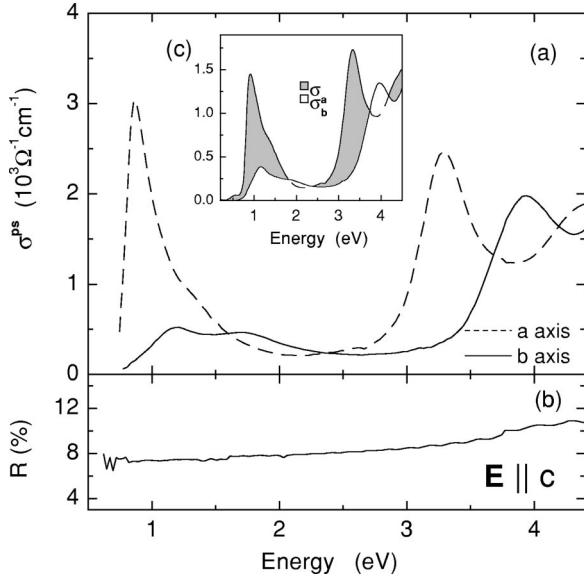
FIG. 1. (a) Pseudo-optical conductivity $\sigma_1^{ps}(\omega)$ of α'-NaV$_2$O$_5$ at $T=300$ K (Ref. 8). The spectra were taken on the (001) surface with a and b axes successively lying in the plane of incidence. (b) $E\|c$ reflectivity at $T=300$ K. (c) Optical conductivity $\sigma_a(\omega)$ and $\sigma_b(\omega)$ corrected for contributions of the c-axis dielectric function to $\sigma_1^{ps}(\omega)$. The label for the y axis of the inset (c) has the same units as for the main panel (a).

planes were available large enough to do ellipsometry with our setup. We therefore measured the c-axis reflectivity [Fig. 1(b)] of the bc plane of the pristine material (sample CR3). The spectrum contains no (or very weak) absorption peaks in the measured frequency range, as it was reported earlier,[9,10] providing a very reliable determination of the dielectric function ϵ_c using Kramers-Kronig analysis. Due to the absence of strong resonances, ϵ_c has a minor influence on the recorded ellipsometric spectra. In Fig. 1(c) the optical conductivity is displayed taking into account all corrections due to the anisotropy. We see that the conversion from $\epsilon^{ps}(\omega)$ to $\epsilon(\omega)$ has indeed a rather small effect on the spectra. In essence it leads to a factor 0.5 rescaling of $\sigma(\omega)$.

The data are in general agreement with previous results[11,12] using Kramers-Kroning analysis of reflectivity data. Along the a direction we observe a peak at 0.9 eV with a shoulder at 1.4 eV, a peak at 3.3 eV, and the slope of a peak above 4.2 eV, outside our spectral window. A similar blue-shifted sequence is observed along the b direction. The 1-eV peak drops rather sharply and extrapolates to zero at 0.7 eV. However, weak absorption has been observed within the entire far and midinfrared range.[10,11] The strong optical absorbtion within the entire visible spectrum causes the characteristic black appearance of this material.

The peak positions appear to be doping independent, but the striking observation is that the *intensity* of the peaks depends strongly on doping. In particular, the measured intensity of the 1-eV peak for the a axis is directly proportional to $1-x$ (Fig. 2). The 1-eV peak for the b axis shows also a decrease upon doping.

IV. MAIN ELEMENTS OF THE ELECTRONIC STRUCTURE

Before entering the interpretation of the data, we need to discuss in some more detail the main elements of the elec-
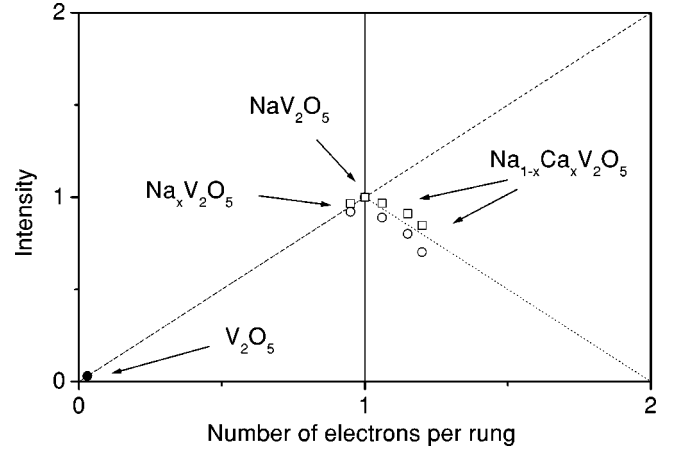

FIG. 2. Intensity of peak A calculated by integrating optical conductivity up to 1.9 eV (squares), or by using the height of the peak (circles) in Ca$_x$Na$_{1-x}$V$_2$O$_5$ for $x=0.06$, $x=0.15$, and $x=20$, and in Na$_x$V$_2$O$_5$ for $x=0.95$. The dashed line indicates the theoretical intensity of in-site Vdd transitions versus doping. The dotted line indicates the theoretical intensity according to the model Hamiltonian Eq. (3).

tronic structure of these compounds. The basic building block of the crystal structure of α'-NaV$_2$O$_5$ is formed by VOV dimers. These dimers form the rungs of quasi-one-dimensional ladders. The V ions forming the rungs are bonded along the ladder direction via oxygen ions.

The backbone of the electronic structure is formed by the oxygen $2p$ and V$3d$ states. Photoelectron spectroscopy[13] has provided crucial information on the occupied electronic levels: The oxygen $2p$ states have the lowest energy (the highest binding energy). They form a band about 4 eV wide, which is fully occupied. The occupied part of the V $3d$ states is located about 3 eV above the top of the oxygen bands. Due to ligand field splittings the V $3d$ manifold is spread over a range of at least 3 eV. The $3d_{xy}$ of the V^{4+} is occupied with one electron. The unoccupied d_{xz} and d_{yz} levels have an energy at least 1 eV higher. These in turn are located about 2 eV below the $d_{x^2-y^2}$ and the d_{z^2} levels.[4] The relevance of the O $2p$ bands is that they provide a path for virtual hopping processes between the V sites. The coupling between V sites is through virtual hopping via π-bonded O $2p_y$ states, indicated schematically in Fig. 4(b). The effective hopping parameter between V sites is $t_\perp \approx -0.3$ eV on the same rung, and $t_\| \approx -0.2$ eV along the legs of the ladder.[14,16,17] The number of electrons is one per pair of V atoms. Approaching the ladders as a linear array of rungs, weakly coupled along the direction of the ladder, results in a model of electrons occupying a narrow band of states formed by the antisymmetric combination of the two V $3d$ states forming the rungs, hereafter referred to as V-V bonding levels.

Hence we see that the basic building block are the pairs of V$3d$ states, together forming the rungs of the ladders. The essential charge and spin degrees of freedom of a single rung are identical to the Heitler-London model of the H$_2^+$ ion, with the V$3d_{xy}$ states playing the role of the H $1s$ states.[14] The relevant Hamiltonion is

$$H=t_\perp \sum_\sigma \{d_{L\sigma}^\dagger d_{R\sigma}+d_{R\sigma}^\dagger d_{L\sigma}\}+\frac{\Delta}{2} \sum_\sigma \{n_{L\sigma}-n_{R\sigma}\}$$

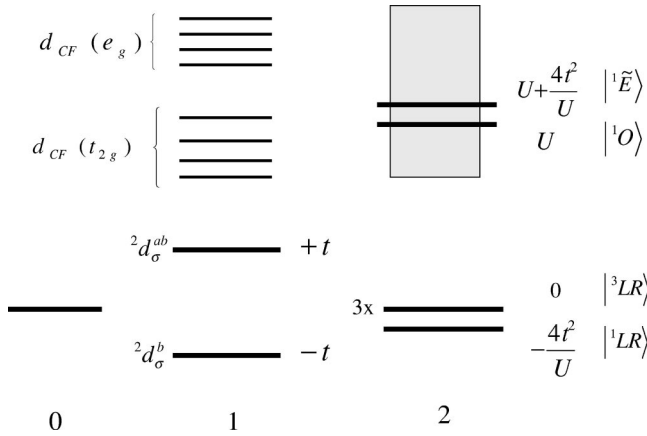$$+U\{n_{L\uparrow}n_{L\downarrow}+n_{R\uparrow}n_{R\downarrow}\}, \qquad (3)$$

FIG. 3. Diagram of the many-body eigenstates of a VOV rung, occupied with 0, 1, and 2 electrons, obtained within the Heitler-London model for $t_\perp/U = 0.1$ and $\Delta = 0$.

where $d^\dagger_{L(R),\sigma}$ creates an electron in the left-hand (right-hand) d_{xy} orbital on the rung, and σ is the spin index. The bias potential Δ between the two V sites accounts for a possible left/right charge imbalance,[11] but the principal conclusions of this paper remain the same, irrespective of its presence. The most relevant states for the ground state are $d_{L,xy}$ and $d_{R,xy}$. Pure NaV_2O_5 contains one electron per rung in the ground state. Important in the present discussion are the eigenstates and energies of a rung with 0, 1, or 2 electrons. The eigenstates and energies are listed in Table I.

In Fig. 3 the level diagram is displayed. In this representation $N_e = 0(2)$ corresponds to the one electron removal (addition) states, for noninteracting electron picture indicated as the ''occupied'' (''empty'') states. In Fig. 4 we display the same information represented as the the one electron removal and addition spectral function. For noninteracting electrons this represents the occupied (left) and unoccupied (right) states.

In the absence of electron-electron interactions, here represented by the on-site Hubbard repulsion parameter U, the Fermi energy would be located in the middle of the bonding
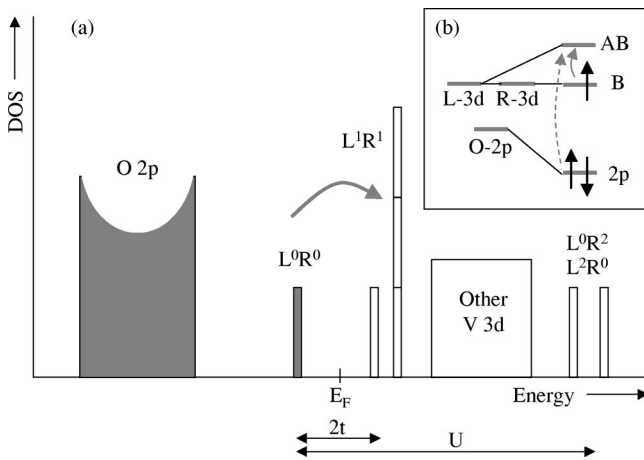

FIG. 4. Occupied and unoccupied density of states obtained within the Heitler-London model for $t_\perp/U = 0.1$ and $\Delta = 0$ (a), and the schematic diagram of the relevant energy levels of the V_2O clusters forming a rung (b). L and R refer to orbitals associated to the left and right V sites, respectively.

band, resulting in a metallic conductor. In Figs. 3 and 4 we have adopted $U = 4$ eV. The model now predicts a gap of order $E_{CT} \simeq 1$ eV. The Fermi energy is located within this gap. The fact that these materials are insulating therefore is associated with the large on-site Hubbard interaction.

The excitation of an electron across the gap involves a change of occupancy of *two* of the rungs: The final state has one empty and one doubly occupied rung. It is important in this context, that the two electrons $|^{3,1}LR\rangle$ are in a *correlated* state: In the limit $U \to \infty$ one electron is located on the left-hand V atom and the other on the right-hand V atom.

V. DISCUSSION OF THE EXPERIMENTAL SPECTRA

The 0.9-eV peak marks the fundamental gap of the optical spectrum. The interpretation of this peak is still subject of a scientific controversy. Several interpretations have been put forward:

(1) Transitions between linear combinations of V $3d_{xy}$ states of the two V ions forming the rungs.[4,14,11] In Refs. 4 and 14 even and odd combinations were considered. The 0.9-eV peak in $\sigma_a(\omega)$ (peak A) would then correspond to the transition from V-V bonding to antibonding combinations on the same rung[11] [Fig. 4(b)]. In Ref. 11 this model was extended to allow lopsided linear combinations of the same orbitals, so that the 0.9-eV peak is a transition between left-and right-oriented linear combinations.

(2) On-site d-d transitions between the crystal field split levels of the V ions.[12] Because V^{5+} has no occupied $3d$-levels, such processes involve the V^{4+} ions. The transitions are allowed because there is no center of inversion.

(3) Transitions between the on-rung V $3d^+_{xy}$ bonding combination and final states of d_{xz} and d_{yz} character.[15]

Optical transitions having values below 2 eV were also seen in V_6O_{13} and VO_2. In V_2O_5 they have very small intensities, and were attributed to defects.[18] The last two assignments are motivated by the fact that in α'-$Na_{1-x}Ca_xV_2O_5$ the optical selection rules allow on-site d-d transitions by virtue of the low point symmetry at the V sites. To determine which one of these assignments is true, we have measured the doping dependence of the 0.9-eV peak in $\sigma_a(\omega)$ in Ca-substituted α'-NaV_2O_5 [Fig. 5(a)]. Because Ca is divalent, substituting Na with Ca has the effect of increasing the average density of V^{4+} ions.

In the local d-d scenario the intensity of the on-site V $3d$-$3d$ transitions would be proportional to the density of V^{4+} ions. As a result the intensity of on-site d-d transitions increases upon substituting Na with Ca. In Fig. 2 we display the experimentally observed doping dependence of the intensity together with the theoretical expectation within this scenario.

Clearly the experimental intensity of the 0.9-eV peak in Fig. 5 behaves opposite to the expected behavior of dd transitions. This definitely rules out item number 2 of the above list.

This also rules out item number 3 presented in Ref. 15: if the transition from the V $3d^+_{xy}$ bonding combination to the d_{xz} and d_{yz} orbitals involves mainly transitions among orbitals at the same site, the same argument as for item 2 applies. If it involves mainly transitions between molecular orbitals formed by different sites on the same rung, the transition

TABLE I. Eigenstates and energies of a rung with $N_e = 0$, 1, and 2 electrons. The $N_e = 2$ state vectors and energies were derived for the limit $\Delta \ll U$.

N_e	State vector	Energy
0	$\|0\rangle$	0
1	$\|{}^2B_\sigma\rangle = (ud^\dagger_{L\sigma} + vd^\dagger_{R\sigma})\|0\rangle$	$-\frac{1}{2}E_{CT} - E_F$
	$\|{}^2A_\sigma\rangle = (vd^\dagger_{L\sigma} - ud^\dagger_{R\sigma})\|0\rangle$	$+\frac{1}{2}E_{CT} - E_F$
2	$\|{}^1\widetilde{LR}\rangle = \alpha_K\|{}^1LR\rangle + \beta_K\|{}^1E\rangle$	$-K - 2E_F$
	$\|{}^3LR_1\rangle = d^\dagger_{L\uparrow}d^\dagger_{R\uparrow}\|0\rangle$	$-2E_F$
	$\|{}^3LR_0\rangle = \sqrt{\frac{1}{2}}(d^\dagger_{L\uparrow}d^\dagger_{R\downarrow} + d^\dagger_{L\downarrow}d^\dagger_{R\uparrow})\|0\rangle$	$-2E_F$
	$\|{}^3LR_{-1}\rangle = d^\dagger_{L\downarrow}d^\dagger_{R\downarrow}\|0\rangle$	$-2E_F$
	$\|{}^1\widetilde{O}\rangle = \alpha_\Delta\|{}^1O\rangle + \beta_\Delta\alpha_K\|{}^1E\rangle - \beta_\Delta\beta_K\|{}^1LR\rangle$	$U + K/2 - \sqrt{(K/2)^2 + \Delta^2} - 2E_F$
	$\|{}^1\widetilde{E}\rangle = \alpha_\Delta\alpha_K\|{}^1E\rangle - \alpha_\Delta\beta_K\|{}^1LR\rangle - \beta_\Delta\|{}^1O\rangle$	$U + K/2 + \sqrt{(K/2)^2 + \Delta^2} - 2E_F$
Definitions	$\dfrac{u}{v} \equiv \sqrt{1 + [\Delta/2t_\perp]^2} + [\Delta/2t_\perp]$	$E_{CT} \equiv \sqrt{4t_\perp^2 + \Delta^2}$
	$\|{}^1LR\rangle \equiv \sqrt{\frac{1}{2}}(d^\dagger_{L\uparrow}d^\dagger_{R\downarrow} - d^\dagger_{L\downarrow}d^\dagger_{R\uparrow})\|0\rangle$	$K \equiv \sqrt{U^2/4 + 4t_\perp^2} - U/2$
	$\|{}^1E\rangle \equiv \sqrt{\frac{1}{2}}(d^\dagger_{L\uparrow}d^\dagger_{L\downarrow} + d^\dagger_{R\uparrow}d^\dagger_{R\downarrow})\|0\rangle$	$\dfrac{\alpha_K}{\beta_K} \equiv \sqrt{1 + [U/4t_\perp]^2} + [U/4t_\perp]$
	$\|{}^1O\rangle \equiv \sqrt{\frac{1}{2}}(d^\dagger_{L\uparrow}d^\dagger_{L\downarrow} - d^\dagger_{R\uparrow}d^\dagger_{R\downarrow})\|0\rangle$	$\dfrac{\alpha_\Delta}{\beta_\Delta} \equiv \sqrt{1 + [K/2\Delta]^2} + [K/2\Delta]$

from the V $3d^+_{xy}$ bonding combination to the antibonding V $3d^-_{xy}$ would still be the dominant transition.

To explain the intensity decrease of about $x\%$ upon substituting $x\%$ of the Na ions with Ca (see Fig. 2), let us have a look at the many-body nature of the ground state and the excited state properties of NaV_2O_5. The rungs which are occupied with two electrons due to the Ca doping will be in the many-body ground state (see Table I) $\|{}^1\widetilde{LR}\rangle$. Due to the dipole selection rules, the optical excitation with the electric field along the rung direction is $\|{}^1\widetilde{LR}\rangle \rightarrow \|{}^1\widetilde{O}\rangle$. The energy to make this excitation is $\frac{1}{2}U + \sqrt{U^2/4 + 4t_\perp^2}$. Hence the effects of Ca doping are (i) to remove the peak at $E_{CT} \approx 1$ eV for the rungs receiving the extra electron, and (ii) to place a new peak at an energy $U \approx 4$ eV. Hence the observed $x\%$ decrease of intensity of the $\|B\rangle \rightarrow \|A\rangle$ transition peak for the $x\%$ Ca-doped sample is in excellent quantitative agreement with the expected value.

Using the tight-binding f-sum rule $\int \sigma(\omega)d\omega = (ed/\hbar)^2 \pi t_\perp/(2V)\langle d^\dagger_{L\sigma}d_{R\sigma} + d^\dagger_{R\sigma}d_{L\sigma}\rangle$ the *intensity* of the $\|{}^1\widetilde{LR}\rangle \rightarrow \|{}^1\widetilde{O}\rangle$ peak relative to the 0.9-eV peak of the singly occupied rungs is (assuming $\Delta = 0$ for a doubly occupied rung):

$$\frac{I(0) + I(2)}{2I(1)} = \frac{\alpha_K\beta_K}{uv} = \sqrt{\frac{1}{1 + (U/4t)^2}} \approx \frac{4t_\perp}{U}. \quad (4)$$

With the parameters relevant to NaV_2O_5 this implies that the $\|{}^1\widetilde{LR}\rangle \rightarrow \|{}^1\widetilde{O}\rangle, \|{}^1\widetilde{E}\rangle$ transitions have factor 2–4 smaller spectal weight than the $\|B\rangle \rightarrow \|A\rangle$ transition. Hence we conclude that only the assigment of item number 1 is consistent
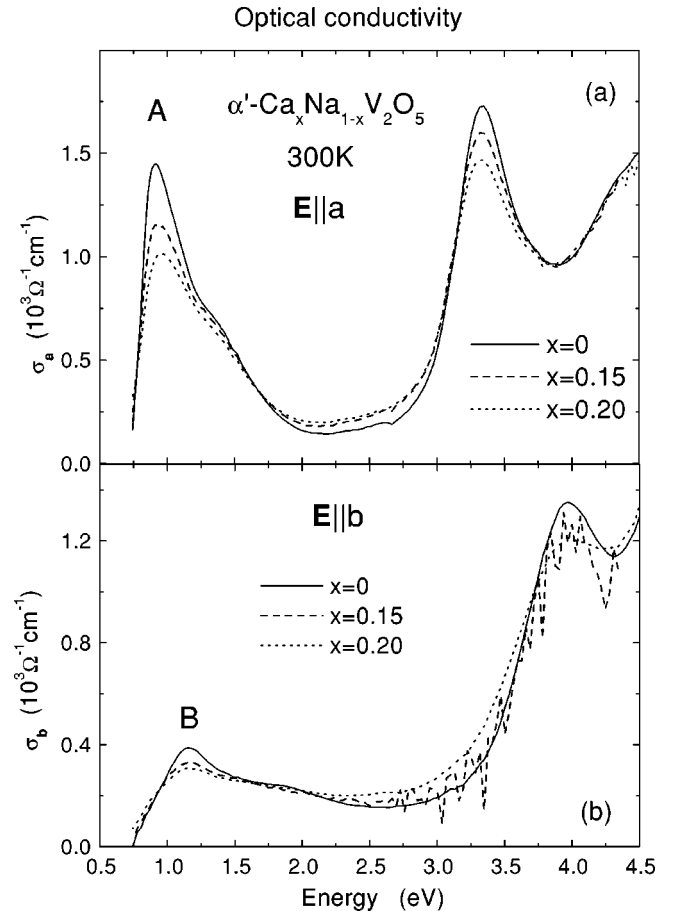

Optical conductivity

FIG. 5. Optical conductivity at $T = 300$ K of Re $\sigma(\omega)$ of $Ca_xNa_{1-x}V_2O_5$ for $x = 0$ (solid), $x = 0.15$ (dash), and $x = 0.20$ (dot): $E\|a$ (panel a) and $E\|b$ (panel b).

with our data: The 1-eV peak in $\sigma_a(\omega)$ is the on-rung $|^2B_\sigma\rangle \rightarrow |^2A_\sigma\rangle$ transition with an excitation energy $E_{CT} \equiv \sqrt{4t_\perp^2 + \Delta^2}$.

The 1.1-eV peak in $\sigma_b(\omega)$ (peak B) involves transitions between neighboring rungs along the ladder. In the noninteracting model ($U=0$) this would correspond to a Drude-Lorentz optical conductivity centered at $\omega=0$, with a spectral weight $\int_0^\infty \sigma_b(\omega)d\omega = (e/\hbar)^2 t_\parallel \pi b (2ac)^{-1}$. As a result of the correlation gap in the density of states, indicated in Fig. 4(a), the optically induced transfer of electrons between neighboring rungs results in a final state with one rung empty, and a neighboring rung doubly occupied, in other words, an electron hole pair consisting of a hole in the band below E_F, and an electron in the empty state above E_F indicated in Fig. 4(a). This corresponds to the process

$$2|^2B_\sigma\rangle \rightarrow |^{3,1}LR\rangle + |0\rangle. \tag{5}$$

Note that the final-state wave function is qualitatively different from the on-rung bonding-antibonding excitations considered above, even though the excitations are close in energy: it involves one rung with no electron, and a neighboring rung with one electron occupying each V atom. The energy of this process is approximately $2t_\perp + \delta V$, where δV represents the increase in Coulomb interaction by bringing two electrons together on the same rung. Since the distance betweeen the electrons changes from about 5.0 to 3.4 Å, and taking into account a screening factor $\epsilon \approx 6$, we estimate that $\delta V \simeq 0.2$ eV.

This value of δV corresponds closely to the difference in peakpositions along the a and b directions. According to this interpretation the absorption at 1.1 eV along b corresponds to the creation of a free electron and hole, capable of carrying electrical currents. The on-rung excitation at 0.9 eV along the a direction is a localized (charge neutral) excitation, in other words, an exciton. In this case the energy of the exciton involves the states of a single electron only, whereas the free carrier states involve many-body interactions.

Doping with Ca creates doubly occupied rungs, whose ground energy is not $2|^2B_\sigma\rangle$ but $|^1\widetilde{LR}\rangle$. Consequently, the electrons on these rungs will not be involved in the processes of Eq. (5), thus decresing the intensity of the B peak upon doping, as seen from Fig. 5(b).

The room-temperature crystal structure has four V atoms per unit cell, organized in ladders with up and down oriented apical oxygens alternating along the a direction, resulting in a double degeneracy of the electronic states discussed above. The coupling between adjacent ladders lifts the degeneracy of these states, resulting in a ''Davidov'' splitting of the peaks A and B. This can create the two additional ''shoulders'' in $\sigma(\omega)$ at 1.4 and 1.7 eV for peaks A and B, respectively.

Photoemission spectroscopy showed that an energy of 3 eV separates the V3d band from the O2p. We therefore attribute the peaks at 3.3 eV in $\sigma_a(\omega)$ and the peak at 4 eV in $\sigma_b(\omega)$ to transitions of the type

$$|^2B_\sigma\rangle \rightarrow |\underline{2p}^1 LR\rangle, \tag{6}$$

where the 2p hole is located on the oxygen on the same rung for peak A, and in between the rungs for peak B. This is further supported by previous optical measurements on V_2O_5 (Ref. 18) which, showed a peak at about 3 eV. In V_2O_5 all V ions have a formal V3d^0 configuration, hence the 3-eV peak cannot be attributed to d-d transitions. However, the O2p $\rightarrow$ V3d transitions should appear at approximately the same photon energy as in NaV_2O_5, which further supports our assigment of the 3-eV peak in NaV_2O_5 to O2$p \rightarrow$ V3d transitions. The observed decrease in the intensity of the 3.3-eV peak for $E\|a$ is explained through the same mechanism which yields the decrease of the 1-eV peak. Upon doping, there are some doubly occupied rungs. If the 3.3-eV peak is a O2$p \rightarrow$ V3d transition, in the doubly occupied rungs it will require an additional Coulomb energy U, and the intensity of the 3.3-eV peak will decrease.

VI. CONCLUSIONS

In conclusion, we have measured the dielectric function along the a and b axes of $Ca_xNa_{1-x}V_2O_5$ for $x=0$, 0.06, 0.15 and $x=0.20$. The 0.9-eV peak in $\sigma_a(\omega)$ was shown experimentally to be a bonding-antibonding transition inside the V_2O rung and not a vanadium d-d transition due to crystal-field splitting. We identified the 3.3-eV peak in $\sigma_a(\omega)$ as the transition from the oxygen orbitals to the antibonding one. This strongly supports the notion, previously expressed in Refs. 4,14, and 11, that NaV_2O_5 is an insulator due to a combination of three factors: a crystal-field splitting, an on-site Hubbard interaction, and an on-rung bonding-antibonding splitting of the two V3d_{xy} orbitals, each of which is large compared to the inter-rung hopping parameter.

ACKNOWLEDGMENTS

[1] J. Galy, J. Solid State Chem. **100**, 229 (1992).

[2] A. Meetsma, J.L. de Boer, A. Damascelli, J. Jegoudez, A. Revcolevschi, and T.T.M. Palstra, Acta Crystallogr., Sect. C: Cryst. Struct. Commun. **C54**, 1558 (1998).

[3] H.G. von Schnering, Yu. Grin, M. Kaupp, M. Somer, R.K. Kremer, and O. Jepsen, Z. Kristallogr. **213**, 246 (1998).

[4] H. Smolinski, C. Gros, W. Weber, U. Peuchert, G. Roth, M. Weiden, and C. Geibel, Phys. Rev. Lett. **80**, 5164 (1998).

[5] M. Isobe, C. Kagami, and Y. Ueda, J. Cryst. Growth **181**, 314 (1997).

[6] R.M.A. Azzam and N.M. Bashara, *Ellipsometry and Polarized Light* (North-Holland, Amsterdam, 1997).

[7] D.E. Aspnes, J. Opt. Soc. Am. **70**, 1275 (1980).

[8] Because $\sigma(\omega)$ is a direct measure of the spectral weight in relation to the f-sum rule, we use $\sigma(\omega)$ as a representation of Im $\epsilon(\omega)$ throughout this paper.

[9] M. Konstantinović, L.F. Lastras-Martinez, M. Cardona, Z.V. Popovic, A.N. Vasilev, M. Isobe, and Y. Ueda, Phys. Status Solidi B **211**, R3 (1999).

[10] D. Smirnov, J. Leotin, P. Millet, J. Jegoudez, and A. Revcolevschi, Physica B **259**, 992 (1999).

[11] A. Damascelli, D. van der Marel, M. Gruninger, C. Presura, T.T.M. Palstra, J. Jegoudez, and A. Revcolevschi, Phys. Rev. Lett. **81**, 918 (1998); A. Damascelli, C. Presura, D. van der Marel, J. Jegoudez, and A. Revcolevschi, Phys. Rev. B **61**, 2535 (2000).

[12] S. Golubchik, M. Isobe, A.N. Ivlev, B.N. Mavrin, M.N. Popova, A.B. Sushkov, Y. Ueda, and A.N. Vasil'ev, J. Phys. Soc. Jpn.

[13] **66**, 4042 (1997); **68**, 318(E) (1999).

[13] K. Kobayashi, T. Mizokawa, A. Fujimori, M. Isobe, and Y. Ueda, Phys. Rev. Lett. **80**, 3121 (1998).

[14] P. Horsch and F. Mack, Eur. Phys. J. B **5**, 367 (1998).

[15] V.C. Long, Z. Zhu, J.L. Musfeldt, X. Wei, H.J. Koo, M.H. Whangbo, J. Jegoudez, and A. Revcolevschi, Phys. Rev. B **60**, 15 721 (1999).

[16] S. Nishimoto and Y. Ohta, J. Phys. Soc. Jpn. **67**, 3679 (1998).

[17] M. Cuoco, P. Horsch, and F. Mack, Phys. Rev. B **60**, R8438 (1999).

[18] N. Kenny, C.R. Kannewurf, and D.H. Whitmore, J. Phys. Chem. Solids **27**, 1237 (1966).